International Journal of Advances in Applied Sciences (IJAAS)
Vol. 13, No. 3, September 2024, pp. 556~565
ISSN: 2252-8814, DOI: 10.11591/ijaas.v13.i3.pp556-565

Optimization of mechanical properties of Al7150/Si3N4/C composites using artificial neural network

Mohamed Zakaulla, Younus Pasha
Department of Mechanical Engineering, HKBK College of Engineering, Visvesvaraya Technological University, Bangalore, India

Article Info

Article history:

Received Dec 27, 2023
Revised May 13, 2024
Accepted May 17, 2024

Keywords:

Aluminum
Artificial neural network
Graphene
Heat treatment
Mechanical property

ABSTRACT

The study aims to investigate and predict the effect of reinforcements such as silicon nitride (Si3N4) and graphene (C) in aluminum 7150 matrix. Al7150/Si3N4/C hybrid composite is fabricated by a stir casting technique and subsequently T6 heat treated for applications such as body stringers, spar chords, seat tracks, and stringers of wing surfaces of aircraft. A feedforward propagation multilayer neural network was developed for modeling and prediction of hardness, tensile strength, and tensile elongation. The results show that the addition of fillers and T6 heat treatment enhances the mechanical properties of the Al7150/Si3N4/C composite. The artificial neural network (ANN) model suggested for Al7150 composites demonstrates beneficial results when compared to experimental measurements. The prediction model, which has a mean absolute percentage error of 0.64%, 0.3%, and 2.49% for hardness, tensile strength, and tensile elongation can accurately predict the effect of reinforcement contents and T6 heat treatment on mechanical properties of Al7150/Si3N4/C composites.

Corresponding Author:

Mohamed Zakaulla
Department of Mechanical Engineering, HKBK College of Engineering
Visvesvaraya Technological University
Bangalore 560045, India
Email: zakaulla.me@hkbk.edu.in

1. INTRODUCTION

Al7150 alloy is widely used in the aerospace industry in manufacturing upper wing stringers, fuselage reinforcement, fixed leading edge, and upper wing structures due to its resistance to fatigue, good ductility, excellent toughness, wear resistance, and resistance to exfoliation corrosion [1]-[5]. Silicon nitride has numerous applications in the aerospace industry such as engine components, radomes, radio frequency (RF) windows, ball bearings, and missile fins due to its extremely high strength of up to 1,200 °C, thermal shock resistance at high temperatures, lightweight and excellent wear resistance [6]-[9]. Graphene is widely used as a cooling system for satellites, cables for space lifts, solar sails, and de-icing systems integrated into wings due to properties such as lightweight, electrical conductivity, excellent thermal properties, and high tensile strength [10]-[15]. Akhtar *et al.* [16] investigated the optimum heat treatment of aluminum alloy AC8H to improve its performance. Hardness, impact, and tensile tests were performed on untreated and heat-treated specimens. Solutionizing was carried out at 530 °C and aged at different temperatures to find the optimal properties. Results indicated that hardness, ultimate tensile strength, yield strength, and impact toughness enhanced to 28 HRA, 177 MPa, 80 MPa, and 5.25 J when specimens were aged at 175 °C. Majeed *et al.* [17] investigated the effect of T4 and T6 heat treatment on AlSi10Mg alloy and the result showed that minimum porosity and best densification is possible at 144.89 J/mm^3 and it was confirmed by scanning electron microscopy (SEM) images of high dense parts have less porosity. Finally, it is concluded that T4 heat treatment at 530 °C enhanced density to 99.94% and T6 heat treatment to 99.87% due to strong bonding among powder particulates. Azadi and Shirazabad [18] investigated the effect of heat treatment on A356 alloy concerning low cycle fatigue used in diesel engine cylinder heads. Heat treatment applied to A356 aluminum alloy is solutionised at 535 °C for 8 h, and then water quenched and later aged for 3 h at 180 °C. It is concluded that the mechanical properties of A356 alloy are improved by T6 heat treatment except for thermal fatigue loading. Artificial neural networks (ANN) are used to deal with complicated problems such as unknown data prediction and analyzing nonlinear systems and it is extensively used in various aspects of materials science including prediction of tribologic [19]-[26] and mechanical properties [27]-[41], This study looked into effects of adding silicon nitride (Si_3N_4) and graphene to Al7150 alloy for manufacturing Al7150/Si_3N_4/C hybrid composite and subsequently providing T6 heat-treatment. while previous studies investigated the effect of adding different reinforcements to Al7150 alloy. However, they did not explicitly address the ideal combination of Si_3N_4 and graphene and also processing parameters using ANN for reliable and high-quality Al7150 composite material.

2. EXPERIMENTAL DETAILS

2.1. Materials and methods

Al7150 is obtained in the form of billet and silicon nitride is obtained in powder form of 20 microns. Graphene is in the form of a black powder having a bulk density of 0.45 g/cm^3, surface area of 130 m^2/g, average lateral dimension of 10 µm, and number of layers 5-10. Composite is fabricated by melting Al7150 ingots at a temperature of 800 °C in an electrical resistance furnace. Reinforcements such as Si_3N_4 and graphene were uniformly mixed using a ball mill for 2 h and later preheated using a micro-oven. Magnesium was added in a small amount (2 wt%) to establish wettability and reduce oxidation during melting. Preheated reinforcements were added during the stirring of molten alloy and composite slurry was stirred at 350 rpm for 5 mins and later poured in a cast iron mold 25 mm outer and 180 mm height. The Al7150/Si_3N_4/C composite was T6 heat-treated i.e., solutionizing at 530 °C for 60 mins, quenched in ice and subsequently aged for 6 h at 175 °C and later cooled in air as shown in Figure 1. The macro-hardness and tensile test of unheated-treated and T6 heat-treated Al7150 composites was determined as per ASTM E10 and ASTM E8 standards for finding ultimate tensile strength and tensile elongation [42].

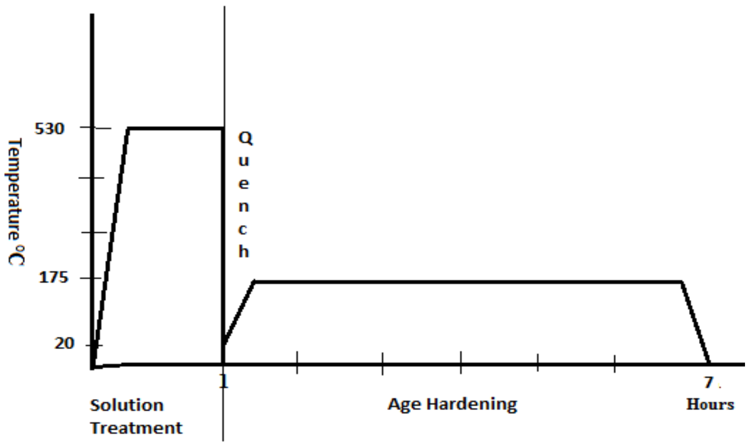

Figure 1. Complete heat treatment cycle

2.2. Artificial neural network

For the present investigation, ANN construction is shown in Figure 2. Table 1 gives an overview of input and output parameters employed for predicting the mechanical properties of untreated and T6 heat-treated Al7150 composites. In the present study, the experimental data were grouped into training (70%) and test data (30%) for examining the effect of reinforcement content and heat treatment on the hardness, tensile strength, and tensile elongation of Al7150 composites. The forecast model was developed with the help of the training data, as shown in Table 2.

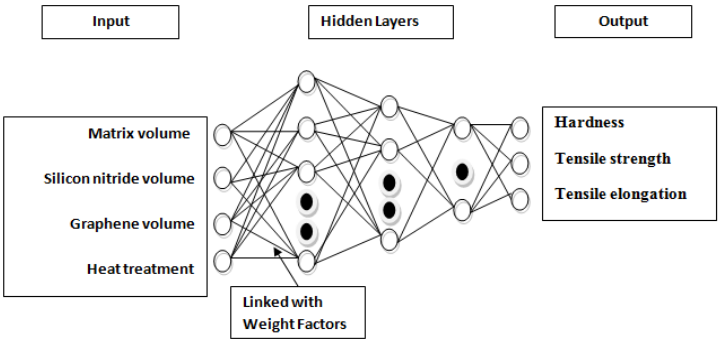

Figure 2. Schematic construction of ANN for correlating material composition and heat treatment with mechanical properties

Table 1. Input and output parameters of ANN

Sl.no	Input parameters	Output parameters
1	Silicon Nitride % (2-4-6-8-10)	Hardness (BHN)
2	Graphene % (0.5-1-1.5-2)	Tensile strength (MPa)
3	Untreated T6 heat- treated	Tensile elongation (%)

Table 2. Experimental data and predicted output from the ANN network for training

Sample ID	Heat treatment	Silicon nitride (Vol %)	Graphene (Vol %)	Hardness (BHN)			Tensile strength (MPa)			Tensile elongation (%)		
				m*	p*	e*	m*	p*	e*	m*	p*	e*
1	Untreated	2	0.5	87.64	87.21	0.49	158.45	158.21	0.15	9.83	9.98	-1.53
2	Untreated	4	0.5	89.02	89.18	-0.18	174.67	174.75	-0.05	9.42	9.47	-0.53
3	Untreated	6	0.5	91.82	91.34	0.52	185.78	185.37	0.22	8.88	8.94	-0.68
4	Untreated	8	0.5	92.54	92.72	-0.19	198.34	198.41	-0.04	7.12	7.29	-2.39
5	Untreated	10	0.5	94.09	94.28	-0.20	216.25	216.52	-0.12	7.68	7.55	1.69
6	Untreated	2	1	89.56	89.14	0.47	162.78	162.96	-0.11	9.16	9.27	-1.20
7	Untreated	4	1	91.11	91.08	0.03	180.34	180.67	-0.18	9.24	9.11	1.41
8	Untreated	6	1	93.27	93.16	0.12	207.72	207.58	0.07	8.46	8.67	-2.48
9	Untreated	8	1	94.75	94.38	0.39	218.98	218.75	0.11	7.05	7.14	-1.28
10	Untreated	10	1	97.82	98.16	-0.35	248.32	248.73	-0.17	7.12	7.29	-2.39
11	Untreated	2	1.5	92.43	92.78	-0.38	170.67	170.39	0.16	8.78	8.61	1.94
12	Untreated	4	1.5	96.27	96.19	0.08	194.67	195.29	-0.32	8.84	8.92	-0.90
13	Untreated	10	1.5	104.43	104.14	0.28	273.64	273.75	-0.04	6.41	6.23	2.81
14	Untreated	10	2	110.76	110.94	-0.16	287.98	287.12	0.30	6.34	6.16	2.84
15	T6	2	0.5	102.72	102.65	0.07	287.26	287.54	-0.10	12.1	12.48	-3.14
16	T6	4	0.5	108.89	108.72	0.16	305.76	306.14	-0.12	11.24	11.56	-2.85
17	T6	6	0.5	112.67	112.32	0.31	347.23	347.95	-0.21	9.23	9.37	-1.52
18	T6	8	0.5	116.65	116.27	0.33	367.56	367.92	-0.10	9.12	9.08	0.44
19	T6	10	0.5	118.72	118.24	0.40	432.74	432.01	0.17	8.42	8.67	-2.97
20	T6	2	1	105.34	105.13	0.20	292.68	292.84	-0.05	11.87	11.83	0.34
21	T6	4	1	113.65	113.58	0.06	334.89	334.27	0.19	10.8	10.88	-0.74
22	T6	6	1	115.64	115.5	0.12	356.43	356.86	-0.12	10.23	10.29	-0.59
23	T6	8	1	120.41	120.48	-0.06	418.67	418.02	0.16	8.68	8.55	1.50
24	T6	10	1	125.25	125.04	0.17	467.34	467.97	-0.13	8.45	8.4	0.59
25	T6	2	1.5	110.76	111.14	-0.34	312.89	312.18	0.23	11.5	11.17	2.87
26	T6	4	1.5	116.65	116.69	-0.03	340.87	340.12	0.22	9.23	9.07	1.73
27	T6	10	1.5	132.33	132.15	0.14	472.45	472.14	0.06	9.27	9.35	-0.86
28	T6	10	2	138.69	138.47	0.16	488.34	488.87	-0.10	9.68	9.77	-0.93
	MAPE			0.23			0.14			1.61		
	RMSE			0.26			0.47			0.16		

m^* measured, p^* predicted, e^* error (%)

In this investigation, the Levenberg Marquardt algorithm was used as the training algorithm, and the sigmoid and rectified linear activation (ReLu) activation transfer functions were employed. Multiple ANN models are constructed by utilizing a training dataset, employing various combinations of hyperparameters such as learning rate, batch size, epoch, and number of hidden layers. The number of hidden layers with neurons was optimized by hyperparameter tuning using random search. The batch size is selected as 64, 128, and 256. A mean absolute percentage error of 0.64%, 0.3%, and 2.49% for hardness, tensile strength, and tensile elongation was achieved by the ReLU activation function in comparison to other activation functions such as sigmoid. Hence, ReLu with 9, 6, and 4 hidden neurons for layers 1, 2, and 3 respectively, with a learning rate of 0.01, batch size 64, and epoch 500, is selected as the final optimized model. The ANN configuration implemented here is of the form 5-[9-6-4]$_3$-3. Figures 3 and 4 compare the predicted and experimental responses of the training and testing database. The correlation factor connected with the training and test dataset is greater than 0.9.

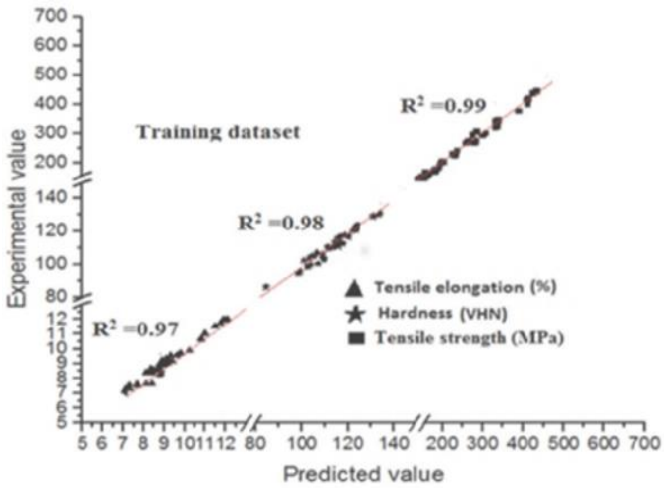

Figure 3. Comparison between the predicted and experimental responses for the training dataset

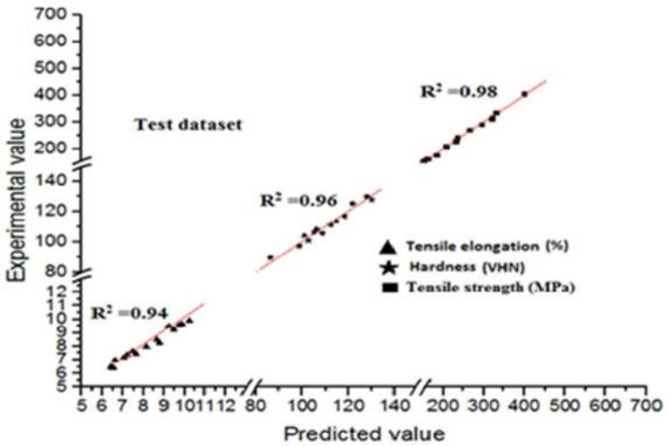

Figure 4. Comparison between the predicted and experimental responses for the test dataset

3. RESULTS AND DISCUSSION

3.1. Modeling results

The predicted values and % error for hardness, tensile strength, and tensile elongation for the training and testing dataset are shown in Tables 2 and 3. The validity of the prediction model was proven using mean absolute percentage error (MAPE) and correlation coefficient from the test dataset as shown in Table 3. The mean absolute percentage error was 0.64% for hardness, 0.3% for tensile strength, and 2.49% for tensile elongation. The results of the ANN model indicate that it is a more accurate and robust predictor of dependent variables than other models [43].

Table 3. Experimental data and predicted output from the ANN network for testing

Sample ID	Heat treatment	Silicon nitride (Vol %)	Graphene (Vol %)	Hardness (BHN)			Tensile strength (MPa)			Tensile elongation (%)		
				m*	p*	e*	m*	p*	e*	m*	p*	e*
1	Untreated	6	1.5	98.68	98.14	0.55	210.89	209.25	0.78	8.41	8.28	1.55
2	Untreated	8	1.5	103.57	104.26	-0.67	240.67	241.14	-0.20	6.84	7.02	-2.63
3	Untreated	2	2	97.82	96.54	1.31	176.28	175.78	0.28	8.34	8.58	-2.88
4	Untreated	4	2	101.05	101.89	-0.83	198.76	198.37	0.20	8.12	7.89	2.83
5	Untreated	6	2	104.43	104.72	-0.28	214.45	215.37	-0.43	7.87	8.09	-2.80
6	Untreated	8	2	108.89	107.56	1.22	243.46	243.82	-0.15	6.78	6.83	-0.74
7	T6	6	1.5	118.72	118.22	0.42	374.34	373.65	0.18	9.62	9.39	2.39
8	T6	8	1.5	126.39	125.12	1.00	436.34	435.09	0.27	8.86	9.02	-1.81
9	T6	2	2	116.65	117.14	-0.42	334.67	335.79	-0.33	10.12	9.74	3.75
10	T6	4	2	121.92	121.53	0.32	354.26	353.41	0.24	9.8	10.06	-2.65
11	T6	6	2	125.25	124.89	0.29	415.346	416.54	-0.29	8.54	8.67	-1.52
12	T6	8	2	131.11	131.78	-0.51	458.64	457.06	0.33	7.3	6.98	4.38
	MAPE			0.64			0.3			2.49		
	RMSE			0.74			1.01			0.22		

m* measured, p* predicted, e* error (%)

3.2. The mechanical properties and heat treatment

Figure 5 shows that the tensile strength enhanced with the addition of reinforcements for Al7150/Si_3N_4/C composite and it is due to Orowan strengthening, mismatch of coefficient of thermal expansion between Al7150 matrix (24 x 10^{-6}/°K), Si_3N_4 particles (3.3 x 10^{-6}/°K) and graphene (-8x10^{-6}/°K) which results in strain hardening of matrix [44]-[48]. Figure 6 shows the hardness of Al7150-based composite and Al7150/10%Si_3N_4/2%C composite showed the highest hardness because of the incorporation of hard Si_3N_4 particles, graphene's hardness resistance, cohesive adhesion between Si_3N_4 particles, graphene, and as well as matrix material [49]-[52]. Tensile elongation shown in Figure 7 decreased with the addition of Si_3N_4 particles and graphene in the untreated Al7150 matrix. However, our findings indicate that higher reinforcement content is not associated with the increase in ductility content of the Al7150 composite. This contrasts with the findings of Liu *et al*. [53] who reported that the inclusion of TiB_2 particles enhanced the ductility of Al-Zn-Mg-Cu matrix composites. We found that the addition of Si_3N_4 and graphene and heat treatment correlate with the increase in mechanical properties. The proposed method in this study, results in inordinately higher tensile and hardness properties of Al7150/Si_3N_4/C composite with heat treatment as compared to properties without heat treatment. This study investigated a comprehensive effect of input parameters such as reinforcement content and heat- treatment on mechanical properties of Al7150/Si_3N_4/C composite. However additional and in-depth research is required to confirm the enhancement of mechanical properties particularly regarding stirring speed, size of reinforcement, melting temperature, stirring time, and pouring temperature.

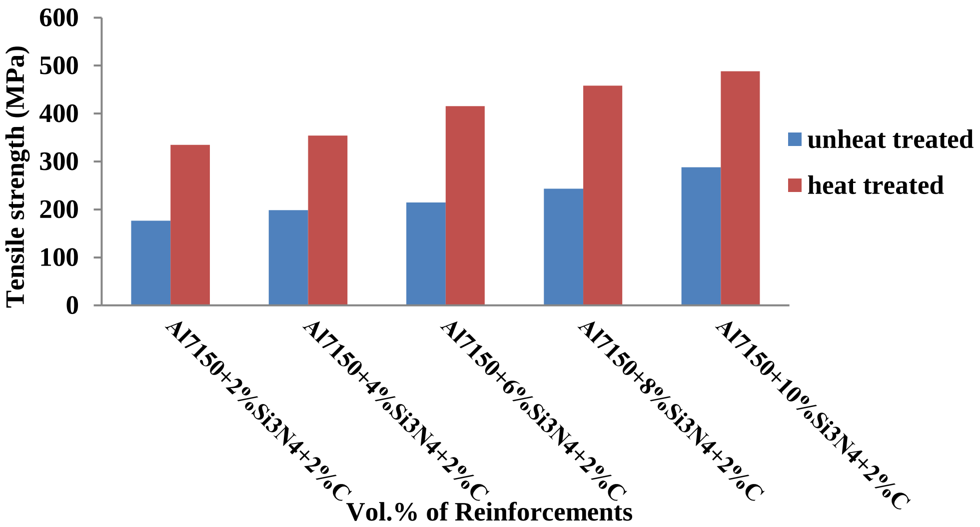

Figure 5. The variation of tensile strength of Al7150/Si_3N_4/C composites with unheated-treated and heat-treated condition

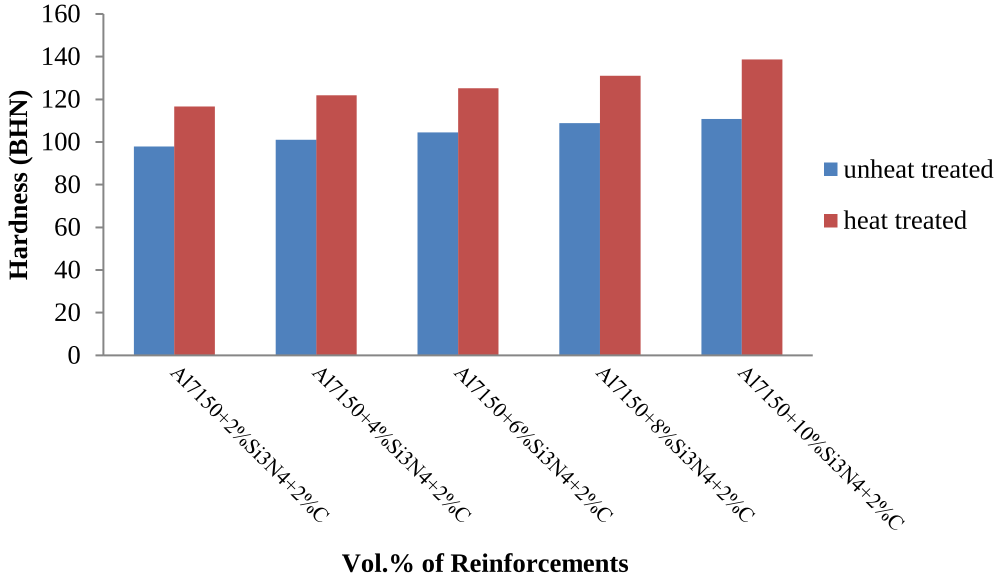

Figure 6. The variation of the hardness of Al7150/Si_3N_4/C composites with unheated treated and heat-treated condition

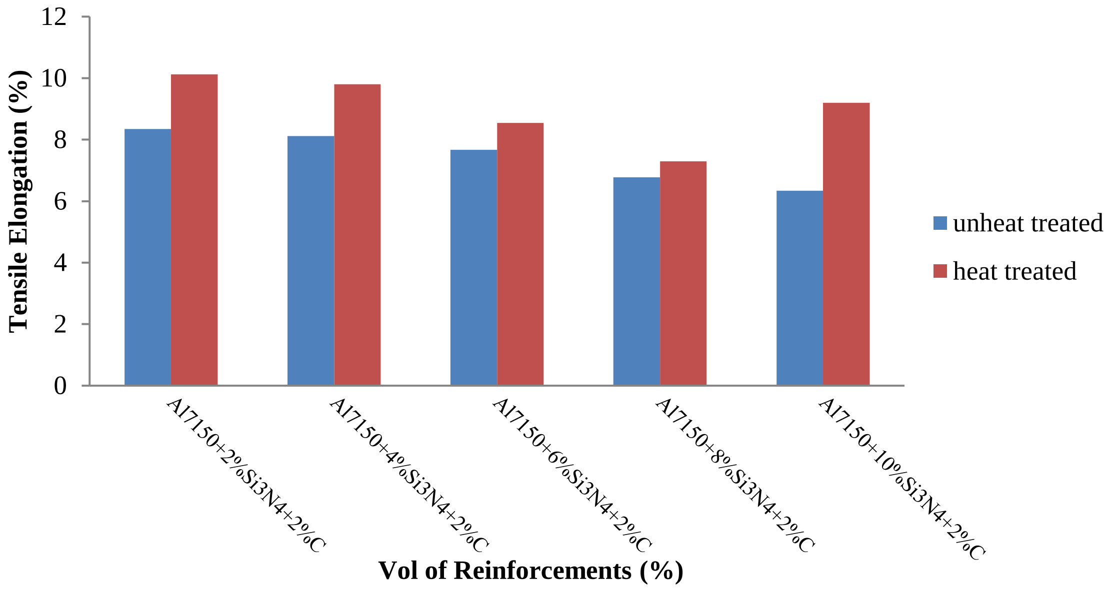

Figure 7. The variation of tensile elongation of Al7150/Si_3N_4/C composites with unheated-treated and heat-treated condition

SEM images of untreated Al7150 composites reinforced with different percentages of reinforcements are shown in Figure 8. It is seen from Figures 8(a) and 8(b) that cracks, voids, and stepwise dendrites occur which is due to the decohesion of silicon nitride particles, and graphene from the matrix which results in brittle fracture. Thus, SEM images of untreated Al7150 composites shown in Figures 8(a) and 8(b) demonstrate brittle fracture due to low wettability and non-uniform distribution of silicon nitride particles. SEM images of T6 heat-treated Al7150 composites shown in Figure 9 (in Figures 9(a) and 9(b) especially) are dominated by a dimple formation which represents ductile fracture due to the improved bonding which is achieved at the interface between the A7150 matrix, Si_3N_4 particles and graphene [54].

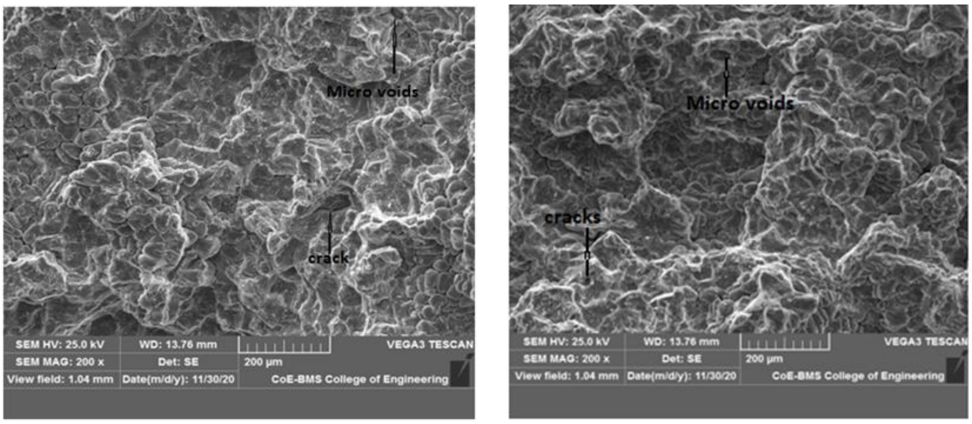

(a) (b)

Figure 8. SEM images of the tensile fracture surface of unheated-treated in (a) Al7150/4%Si_3N_4/2%C and (b) Al7150/8%Si_3N_4/2%C

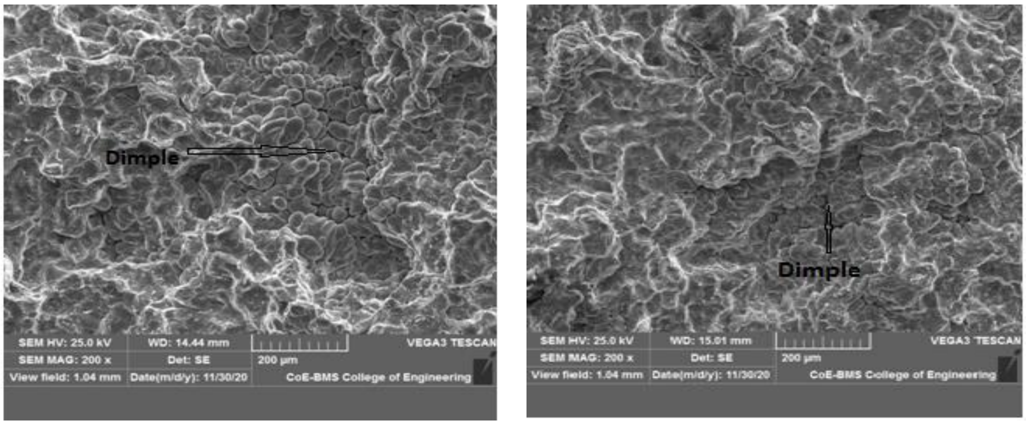

(a) (b)

Figure 9. SEM images of the tensile fracture surface of heat-treated (a) Al7150/4%Si_3N_4/2%C and (b) Al7150/8%Si_3N_4/2%C

4. CONCLUSION

This study indicates that the enhancement of hardness and tensile strength is due to the heat treatment and addition of Si_3N_4 and graphene to Al7150 alloy. Our results offer definite proof that good bonding and cohesive adhesion between Si_3N_4 particles, graphene, and as well as matrix material results in the enhancement of mechanical properties. With T6 heat treatment on Al7150 composites, the mechanical properties of Al7150/Si_3N_4/C composites possess enhanced hardness (138.69 BHN), tensile strength (488.34 MPa), and elongation (12.10%) which makes it a better candidate than the as-cast Al7150 composites. Finally, our research shows that the T6 heat-treatment technique applied to Al7150/Si_3N_4/C composite is more resilient than untreated. Future research may look into additive manufacturing, strain hardening, and extrusion that contribute to the enhancement of the mechanical properties of Al7150 composite. The influence of reinforcement contents and T6 heat treatment on mechanical characteristics of Al7150/Si_3N_4/C composites can be accurately predicted using the prediction model, with a mean absolute percentage error of approximately 2.5% for the predicted values. SEM image of T6 heat-treated Al7150 composites is dominated by a dimple formation which represents ductile fracture and good bonding between the A7150 matrix, Si_3N_4 particles, and graphene.

REFERENCES

[1] P. Madhukar, N. Selvaraj, C. S. P. Rao, and G. B. Veeresh Kumar, “Fabrication and characterization two step stir casting with ultrasonic assisted novel AA7150-hBN nanocomposites,” *J. Alloys Compd.*, vol. 815, p. 152464, Jan. 2020, doi: 10.1016/j.jallcom.2019.152464.

[2] C. Shi and X.-G. Chen, "Evolution of activation energies for hot deformation of 7150 aluminum alloys with various Zr and V additions," *Mater. Sci. Eng. A*, vol. 650, pp. 197–209, Jan. 2016, doi: 10.1016/j.msea.2015.09.105.
[3] X. Fan, D. Jiang, Q. Meng, Z. Lai, and X. Zhang, "Characterization of precipitation microstructure and properties of 7150 aluminium alloy," *Mater. Sci. Eng. A*, vol. 427, no. 1–2, pp. 130–135, Jul. 2006, doi: 10.1016/j.msea.2006.04.043.
[4] M. A. Rahman and N. Sirajudeen, "Influence of aging, varying particle size & volume fraction of Al 2 O 3 particles on the hardness and wear behavior of Al 7150 alloy composite produced by hot uniaxial compaction method," *Mater. Res. Express*, vol. 6, no. 3, p. 35006, Dec. 2018, doi: 10.1088/2053-1591/aaf2c9.
[5] K. Krishnapillai, R. Jones, and D. Peng, "Fatigue based three-dimensional structural design optimisation studies implementing the generalised Frost–Dugdale crack growth law," *Theor. Appl. Fract. Mech.*, vol. 50, no. 1, pp. 30–48, Aug. 2008, doi: 10.1016/j.tafmec.2008.04.008.
[6] C. Zhang *et al.*, "Microstructure and mechanical properties of aluminum matrix composites reinforced with pre-oxidized $β$$-Si3N4 whiskers," *Mater. Sci. Eng. A*, vol. 723, pp. 109–117, Apr. 2018, doi: 10.1016/j.msea.2018.03.038.
[7] P. Sharma, S. Sharma, and D. Khanduja, "Production and some properties of Si 3 N 4 reinforced aluminium alloy composites," *J. Asian Ceram. Soc.*, vol. 3, no. 3, pp. 352–359, Sep. 2015, doi: 10.1016/j.jascer.2015.07.002.
[8] H. Fernández, S. Ordoñez, H. Pesenti, R. E. González, and M. Leoni, "Microstructure homogeneity of milled aluminum A356–Si3N4 metal matrix composite powders," *J. Mater. Res. Technol.*, vol. 8, no. 3, pp. 2969–2977, May 2019, doi: 10.1016/j.jmrt.2019.05.004.
[9] M. Irfan Ul Haq and A. Anand, "Microhardness studies on Stir Cast AA7075-Si3N4 Based Composites," *Mater. Today Proc.*, vol. 5, no. 9, pp. 19916–19922, 2018, doi: 10.1016/j.matpr.2018.06.357.
[10] J. Zhang *et al.*, "Orentational effect of graphene on the friction and wear behavior of Si3N4/TiC based composite ceramic tool materials," *Ceram. Int.*, vol. 46, no. 3, pp. 3550–3557, Feb. 2020, doi: 10.1016/j.ceramint.2019.10.072.
[11] M. Khoshghadam-Pireyousefan, R. Rahmanifard, L. Orovcik, P. Švec, and V. Klemm, "Application of a novel method for fabrication of graphene reinforced aluminum matrix nanocomposites: Synthesis, microstructure, and mechanical properties," *Mater. Sci. Eng. A*, vol. 772, p. 138820, Jan. 2020, doi: 10.1016/j.msea.2019.138820.
[12] B. Xiong, K. Liu, W. Xiong, X. Wu, and J. Sun, "Strengthening effect induced by interfacial reaction in graphene nanoplatelets reinforced aluminum matrix composites," *J. Alloys Compd.*, vol. 845, p. 156282, Dec. 2020, doi: 10.1016/j.jallcom.2020.156282.
[13] A. Bhadauria, L. K. Singh, S. K. Nayak, and T. Laha, "Tensile deformation behavior and strengthening mechanism in graphene nanoplatelet reinforced bimodal grained aluminum nanocomposite synthesized by spark plasma sintering and hot rolling," *Mater. Charact.*, vol. 168, p. 110568, Oct. 2020, doi: 10.1016/j.matchar.2020.110568.
[14] R. Guan *et al.*, "Fabrication of aluminum matrix composites reinforced with Ni-coated graphene nanosheets," *Mater. Sci. Eng. A*, vol. 754, pp. 437–446, Apr. 2019, doi: 10.1016/j.msea.2019.03.068.
[15] P.-X. Zhang, H. Yan, W. Liu, X.-L. Zou, and B.-B. Tang, "Effect of T6 Heat Treatment on Microstructure and Hardness of Nanosized Al2O3 Reinforced 7075 Aluminum Matrix Composites," *Metals (Basel).*, vol. 9, no. 1, p. 44, Jan. 2019, doi: 10.3390/met9010044.
[16] M. Akhtar, S. Z. Qamar, M. Muhammad, and A. Nadeem, "Optimum heat treatment of aluminum alloy used in manufacturing of automotive piston components," *Mater. Manuf. Process.*, vol. 33, no. 16, pp. 1874–1880, Dec. 2018, doi: 10.1080/10426914.2018.1512128.
[17] A. Majeed, Y. Zhang, J. Lv, T. Peng, Z. Atta, and A. Ahmed, "Investigation of T4 and T6 heat treatment influences on relative density and porosity of AlSi10Mg alloy components manufactured by SLM," *Comput. Ind. Eng.*, vol. 139, p. 106194, Jan. 2020, doi: 10.1016/j.cie.2019.106194.
[18] M. Azadi and M. M. Shirazabad, "Heat treatment effect on thermo-mechanical fatigue and low cycle fatigue behaviors of A356.0 aluminum alloy," *Mater. Des.*, vol. 45, pp. 279–285, Mar. 2013, doi: 10.1016/j.matdes.2012.08.066.
[19] A. Kurdi, N. Alhazmi, H. Alhazmi, and T. Tabbakh, "Practice of Simulation and Life Cycle Assessment in Tribology—A Review," *Materials (Basel).*, vol. 13, no. 16, p. 3489, Aug. 2020, doi: 10.3390/ma13163489.
[20] M. Hayajneh, A. M. Hassan, A. Alrashdan, and A. T. Mayyas, "Prediction of tribological behavior of aluminum–copper based composite using artificial neural network," *J. Alloys Compd.*, vol. 470, no. 1–2, pp. 584–588, Feb. 2009, doi: 10.1016/j.jallcom.2008.03.035.
[21] S. Anand Kumar, S. Ganesh Sundara Raman, T. S. N. Sankara Narayanan, and R. Gnanamoorthy, "Prediction of fretting wear behavior of surface mechanical attrition treated Ti–6Al–4V using artificial neural network," *Mater. Des.*, vol. 49, pp. 992–999, Aug. 2013, doi: 10.1016/j.matdes.2013.02.076.
[22] M. Kannaiyan, G. Karthikeyan, and J. G. Thankachi Raghuvaran, "Prediction of specific wear rate for LM25/ZrO2 composites using Levenberg–Marquardt backpropagation algorithm," *J. Mater. Res. Technol.*, vol. 9, no. 1, pp. 530–538, Jan. 2020, doi: 10.1016/j.jmrt.2019.10.082.
[23] S. Gangwar and V. K. Pathak, "Dry sliding wear characteristics evaluation and prediction of vacuum casted marble dust (MD) reinforced ZA-27 alloy composites using hybrid improved bat algorithm and ANN," *Mater. Today Commun.*, vol. 25, p. 101615, Dec. 2020, doi: 10.1016/j.mtcomm.2020.101615.
[24] D. Aleksendrić, D. C. Barton, and B. Vasić, "Prediction of brake friction materials recovery performance using artificial neural networks," *Tribol. Int.*, vol. 43, no. 11, pp. 2092–2099, Nov. 2010, doi: 10.1016/j.triboint.2010.05.013.
[25] S. D. S. Abhiram Kalvakolanu, S. K. P. Kolluru, U. M. R. Paturi, and A. R. Patil, "Modelling erosive wear of nano-filler added carbon fibre reinforced polymer composite by artificial neural networks," *Mater. Today Proc.*, Feb. 2023, doi: 10.1016/j.matpr.2023.01.203.
[26] L. Natrayan and M. S. Kumar, "Optimization of wear parameters of aluminium hybrid metal matrix composites by squeeze casting using Taguchi and artificial neural network," in *Sustainable Manufacturing and Design*, Elsevier, 2021, pp. 223–234. doi: 10.1016/B978-0-12-822124-2.00010-X.
[27] S. Singhal, S. Ahmad Khan, M. Muaz, and E. Ahmed, "Simulation of mechanical properties of stir cast aluminum matrix composites through Artificial Neural Networks (ANN)," *Mater. Today Proc.*, vol. 72, pp. 1102–1109, 2023, doi: 10.1016/j.matpr.2022.09.174.
[28] A. Sheelwant, P. M. Jadhav, and S. K. R. Narala, "ANN-GA based parametric optimization of Al-TiB2 metal matrix composite material processing technique," *Mater. Today Commun.*, vol. 27, p. 102444, Jun. 2021, doi: 10.1016/j.mtcomm.2021.102444.
[29] M.-K. Kazi, F. Eljack, and E. Mahdi, "Optimal filler content for cotton fiber/PP composite based on mechanical properties using artificial neural network," *Compos. Struct.*, vol. 251, p. 112654, Nov. 2020, doi: 10.1016/j.compstruct.2020.112654.
[30] M. Karbalaei Akbari, K. Shirvanimoghaddam, Z. Hai, S. Zhuiykov, and H. Khayyam, "Nano TiB2 and TiO2 reinforced composites: A comparative investigation on strengthening mechanisms and predicting mechanical properties via neural network modeling," *Ceram. Int.*, vol. 43, no. 18, pp. 16799–16810, Dec. 2017, doi: 10.1016/j.ceramint.2017.09.077.
[31] K. Shirvanimoghaddam *et al.*, "Boron carbide reinforced aluminium matrix composite: Physical, mechanical characterization and

mathematical modelling," *Mater. Sci. Eng. A*, vol. 658, pp. 135–149, Mar. 2016, doi: 10.1016/j.msea.2016.01.114.
[32] R. Esmaeili and M. R. Dashtbayazi, "Modeling and optimization for microstructural properties of Al/SiC nanocomposite by artificial neural network and genetic algorithm," *Expert Syst. Appl.*, vol. 41, no. 13, pp. 5817–5831, Oct. 2014, doi: 10.1016/j.eswa.2014.03.038.
[33] M. O. Shabani and A. Mazahery, "Artificial Intelligence in numerical modeling of nano sized ceramic particulates reinforced metal matrix composites," *Appl. Math. Model.*, vol. 36, no. 11, pp. 5455–5465, Nov. 2012, doi: 10.1016/j.apm.2011.12.059.
[34] C. Herriott and A. D. Spear, "Predicting microstructure-dependent mechanical properties in additively manufactured metals with machine- and deep-learning methods," *Comput. Mater. Sci.*, vol. 175, p. 109599, Apr. 2020, doi: 10.1016/j.commatsci.2020.109599.
[35] J. Chen and Y. Liu, "Fatigue modeling using neural networks: A comprehensive review," *Fatigue Fract. Eng. Mater. Struct.*, vol. 45, no. 4, pp. 945–979, Apr. 2022, doi: 10.1111/ffe.13640.
[36] D.-S. Kwon, C. Jin, and M. Kim, "Prediction of dynamic and structural responses of submerged floating tunnel using artificial neural network and minimum sensors," *Ocean Eng.*, vol. 244, p. 110402, Jan. 2022, doi: 10.1016/j.oceaneng.2021.110402.
[37] C. B. Li and J. Choung, "Fatigue damage analysis for a floating offshore wind turbine mooring line using the artificial neural network approach," *Ships Offshore Struct.*, vol. 12, no. sup1, pp. S288--S295, Mar. 2017, doi: 10.1080/17445302.2016.1254522.
[38] T. Varol, A. Canakci, and S. Ozsahin, "Prediction of effect of reinforcement content, flake size and flake time on the density and hardness of flake AA2024-SiC nanocomposites using neural networks," *J. Alloys Compd.*, vol. 739, pp. 1005–1014, Mar. 2018, doi: 10.1016/j.jallcom.2017.12.256.
[39] M. K. Akbari, K. Shirvanimoghaddam, Z. Hai, S. Zhuiykov, and H. Khayyam, "Al-TiB2 micro/nanocomposites: Particle capture investigations, strengthening mechanisms and mathematical modelling of mechanical properties," *Mater. Sci. Eng. A*, vol. 682, pp. 98–106, Jan. 2017, doi: 10.1016/j.msea.2016.11.034.
[40] A. Canakci, T. Varol, and S. Ozsahin, "Artificial neural network to predict the effect of heat treatment, reinforcement size, and volume fraction on AlCuMg alloy matrix composite properties fabricated by stir casting method," *Int. J. Adv. Manuf. Technol.*, vol. 78, no. 1–4, pp. 305–317, Apr. 2015, doi: 10.1007/s00170-014-6646-1.
[41] C. C. Nwobi-Okoye and B. Q. Ochieze, "Age hardening process modeling and optimization of aluminum alloy A356/Cow horn particulate composite for brake drum application using RSM, ANN and simulated annealing," *Def. Technol.*, vol. 14, no. 4, pp. 336–345, Aug. 2018, doi: 10.1016/j.dt.2018.04.001.
[42] "Standard Test Method for Tension Testing of Metallic Materials." ASTM International, 2004.
[43] A. Khamparia, B. Pandey, D. K. Pandey, D. Gupta, A. Khanna, and V. H. C. de Albuquerque, "Comparison of RSM, ANN and Fuzzy Logic for extraction of Oleonolic Acid from Ocimum sanctum," *Comput. Ind.*, vol. 117, p. 103200, May 2020, doi: 10.1016/j.compind.2020.103200.
[44] D. Dunand and A. Mortensen, "Thermal mismatch dislocations produced by large particles in a strain-hardening matrix," *Mater. Sci. Eng. A*, vol. 135, pp. 179–184, Mar. 1991, doi: 10.1016/0921-5093(91)90557-4.
[45] A. Şahin and F. Sarioğlu, "Effect of reinforcements on precipitation behaviour in Al 7075/TiCp composite," *Scr. Mater.*, vol. 37, no. 8, pp. 1117–1121, Oct. 1997, doi: 10.1016/S1359-6462(97)00238-8.
[46] N. Mahathaninwong, T. Plookphol, J. Wannasin, and S. Wisutmethangoon, "T6 heat treatment of rheocasting 7075 Al alloy," *Mater. Sci. Eng. A*, vol. 532, pp. 91–99, Jan. 2012, doi: 10.1016/j.msea.2011.10.068.
[47] A. Albiter, C. A. León, R. A. L. Drew, and E. Bedolla, "Microstructure and heat-treatment response of Al-2024/TiC composites," *Mater. Sci. Eng. A*, vol. 289, no. 1–2, pp. 109–115, Sep. 2000, doi: 10.1016/S0921-5093(00)00900-X.
[48] Li, Yan, Wang, Li, Liu, and Nie, "Effect of Heat Treatment on the Microstructure and Mechanical Properties of a Composite Made of Al-Si-Cu-Mg Aluminum Alloy Reinforced with SiC Particles," *Metals (Basel).*, vol. 9, no. 11, p. 1205, Nov. 2019, doi: 10.3390/met9111205.
[49] P. K. Rohatgi, F. M. Yarandi, and Y. Liu, *Proceedings of International Symposium on Advances in Cast Reinforced Metal Composites*. ASM International Publication, 1998.
[50] Z. Wang *et al.*, "Microstructure and mechanical behavior of metallic glass fiber-reinforced Al alloy matrix composites," *Sci. Rep.*, vol. 6, no. 1, p. 24384, Apr. 2016, doi: 10.1038/srep24384.
[51] C. Chen, L. Guo, J. Luo, J. Hao, Z. Guo, and A. A. Volinsky, "Aluminum powder size and microstructure effects on properties of boron nitride reinforced aluminum matrix composites fabricated by semi-solid powder metallurgy," *Mater. Sci. Eng. A*, vol. 646, pp. 306–314, Oct. 2015, doi: 10.1016/j.msea.2015.08.081.
[52] S. Seetharaman, J. Subramanian, K. Tun, A. Hamouda, and M. Gupta, "Synthesis and Characterization of Nano Boron Nitride Reinforced Magnesium Composites Produced by the Microwave Sintering Method," *Materials (Basel).*, vol. 6, no. 5, pp. 1940–1955, May 2013, doi: 10.3390/ma6051940.
[53] J. Liu *et al.*, "Simultaneously increasing strength and ductility of nanoparticles reinforced Al composites via accumulative orthogonal extrusion process," *Mater. Res. Lett.*, vol. 6, no. 8, pp. 406–412, Aug. 2018, doi: 10.1080/21663831.2018.1471421.
[54] Z. Yuan *et al.*, "Effect of heat treatment on the interface of high-entropy alloy particles reinforced aluminum matrix composites," *J. Alloys Compd.*, vol. 822, p. 153658, May 2020, doi: 10.1016/j.jallcom.2020.153658.

BIOGRAPHIES OF AUTHORS

Dr. Mohamed Zakaulla has completed his Ph.D. in Mechanical Engineering with a specialization in advanced composite materials from Ghousia College of Engineering affiliated with Visvesvaraya Technological University, Belgaum, India. He has about 17 years of teaching and research experience. Now he is working as a Professor in the Department of Mechanical Engineering at HKBK College of Engineering, Bangalore, India. He has authored over 30 technical articles in refereed journals and conference proceedings. His areas of expertise include material science, tribology, fiber metal laminates, high-performance polymer composites, and artificial neural networks. He is a Lifetime member of MISTE. He can be contacted at email: zakaulla.me@hkbk.edu.in.

Dr. Younus Pasha has completed his Ph.D. in Mechanical Engineering with a specialization in thermal sciences from JSS Academy of Technical Engineering Bangalore affiliated with Visvesvaraya Technological University Belgaum India. He has about 10 years of teaching and research experience. Now he is working as an Associate Professor in the Department of Mechanical Engineering at HKBK College of Engineering, Bangalore, India. Authored a textbook "Fuelling the Future: Biodiesel" and 17 research publications in distinguished journals, received 5 grants from AICTE, VTU, and KSCST. His areas of expertise include Biofuels, Fluid mechanics, Material science, Vibrational analysis, Design for manufacturing, and Mechatronics. He is a Lifetime member of MISTE. He can be contacted at email: younuspashame@gmail.com.